Figure 4: Upwind-biased stencils for faces far away from the boundaries of two-dimensional (a) triangular, (b) rectangular and (c) hexagon meshes. The stencil is used to fit a multidimensional polynomial to cell centre values, ϕ_c, marked by grey circles, in order to approximate the value ϕ_F at the face centroid marked by an open circle. ϕ_u and ϕ_d are the values at the centroids of the upwind and downwind cells neighbouring the target face, drawn with a heavy line. The wind vector $\mathbf{u}_f$ is prescribed at face f and determines the choice of stencil at each timestep.

3 Multidimensional advection scheme

The advection of a dependent variable ϕ is given by the conservation equation

$$\frac{\partial \phi}{\partial t} + \nabla \cdot (\mathbf{u}\phi) = 0 \tag{1}$$

where $\mathbf{u}$ is a prescribed wind field. The time derivative is discretised using a three-stage, second-order Runge-Kutta scheme:

$$\phi^\star = \phi^{(n)} + \Delta t f(\phi^{(n)}) \tag{2a}$$

$$\phi^{\star\star} = \phi^{(n)} + \frac{\Delta t}{2}\left(f(\phi^{(n)}) + f(\phi^\star)\right) \tag{2b}$$

$$\phi^{(n+1)} = \phi^{(n)} + \frac{\Delta t}{2}\left(f(\phi^{(n)}) + f(\phi^{\star\star})\right) \tag{2c}$$

where $f(\phi^{(n)}) = -\nabla \cdot (\mathbf{u}\phi^{(n)})$ at time level n.

Using the finite volume method, the wind field is prescribed at face centroids and the dependent variable is stored at cell centroids. The divergence term in equation (1) is discretised using Gauss's theorem:

$$\nabla \cdot (\mathbf{u}\phi) \approx \frac{1}{\mathcal{V}_c} \sum_{f \in c} \mathbf{u}_f \cdot \mathbf{S}_f \phi_F \tag{3}$$

where $\mathcal{V}_c$ is the cell volume, $\mathbf{u}_f$ is a wind vector prescribed at a face, $\mathbf{S}_f$ is the surface area vector with a direction outward normal to the face and a magnitude equal to the face area, and $\sum_{f \in c}$ denotes a summation over all faces f bordering cell c. The value of the dependent variable at the face, ϕ_F, is approximated by a least squares fit over a stencil of surrounding cell centre values.

To introduce the approximation method, we will consider how an approximate value is calculated for a face that is far away from the boundaries of a two-dimensional uniform rectangular mesh. For any mesh, every interior face connects two adjacent cells. The wind direction at the face determines which of the two adjacent cells is the upwind cell. Since the stencil is upwind-biased, two stencils must be constructed for every interior face, and the appropriate stencil is chosen for each face depending on the wind direction at that face for every timestep.

3

The upwind-biased stencil for a face f is shown in figure 4b. The wind at the face, $\mathbf{u}_f$, is blowing from the upwind cell c_u to the downwind cell c_d. To obtain an approximate value at f, a polynomial least squares fit is calculated using the stencil values. The stencil has 4 points in x and 3 points in y, leading to a natural choice of polynomial that is cubic in x and quadratic in y:

$$\phi = a_1 + a_2 x + a_3 y + a_4 x^2 + a_5 xy + a_6 y^2 + a_7 x^3 + a_8 x^2 y + a_9 xy^2 \tag{4}$$

A least squares approach is needed because the system of equations is overconstrained, with 12 stencil values but only 9 polynomial terms. If the stencil geometry is expressed in a local coordinate system with the face centroid as the origin, then the approximated value ϕ_F is equal to the constant coefficient a_1.

The remainder of this section generalises the approximation technique for arbitrary meshes and describes the methods for constructing stencils, performing a least squares fit with a suitable polynomial, and ensuring numerical stability of the advection scheme.

3.1 Stencil construction

For every interior face, two stencils are constructed, one for each of the possible upwind cells. For a given face f and upwind cell c_u, we find those faces that are connected to c_u and 'oppose' face f. These are called the *opposing faces*. The opposing faces for face f and upwind cell c_u are determined as follows. Defining G to be the set of faces other than f that border cell c_u, we calculate the 'opposedness', Opp, between faces f and $g \in G$, defined as

$$\text{Opp}(f, g) \equiv -\frac{\mathbf{S}_f \cdot \mathbf{S}_g}{|\mathbf{S}_f|^2} \tag{5}$$

where $\mathbf{S}_f$ and $\mathbf{S}_g$ are the surface area vectors pointing outward from cell c_u for faces f and g respectively. Using the fact that $\mathbf{a} \cdot \mathbf{b} = |\mathbf{a}|\,|\mathbf{b}|\cos(\theta)$ we can rewrite equation (5) as

$$\text{Opp}(f, g) = -\frac{|\mathbf{S}_g|}{|\mathbf{S}_f|}\cos(\theta) \tag{6}$$

where θ is the angle between faces f and g. In this form, it can be seen that Opp is a measure of the relative area of g and how closely it parallels face f.

The set of opposing faces, OF, is a subset of G, comprising those faces with Opp ≥ 0.5, and the face with the maximum opposedness. Expressed in set notation, this is

$$\text{OF}(f, c_u) \equiv \{g : \text{Opp}(f, g) \geq 0.5\} \cup \{g : \max_{g \in G}(\text{Opp}(f, g))\} \tag{7}$$

On a rectangular mesh, there is always one opposing face that is exactly parallel to the face f.

Once the opposing faces have been determined, the set of internal and external cells must be found. The *internal cells* are those cells that are connected to the opposing faces. Note that c_u is always an internal cell. The *external cells* are those cells that share vertices with the internal cells. Note that c_d is always an external cell. Having found these two sets of cells, the stencil is constructed to comprise all internal and external cells.

Figure 5 illustrates a stencil construction for face f connecting upwind cell c_u and downwind cell c_d. The two opposing faces are denoted by thick dashed lines and the centres of the three adjoining internal cells are marked by black circles. The stencil is extended outwards by including the external cells that share vertices with the internal cells, where the vertices are marked by black squares. The resultant stencil contains 13 cells.

3.2 Least squares fit

To approximate the value at a face f, a least squares fit is calculated from a stencil of surrounding cell centre values. First, we will show how a polynomial least squares fit is calculated for a face on a rectangular mesh. Second, we will make modifications to the least squares fit that are necessary for numerical stability. Finally, we will describe how the approach is applicable to faces of arbitrary meshes.
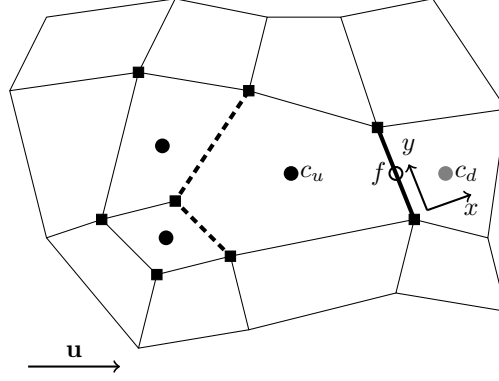
Figure 5: A thirteen-cell, upwind-biased stencil for face f connecting the pentagonal upwind cell, c_u, and the downwind cell c_d. The dashed lines denote the two faces of cell c_u that oppose f, and black circles mark the centroids of the internal cells that are connected to these two opposing faces. The stencil is extended outwards by including cells that share vertices with the three internal cells, where black squares mark these vertices. The local coordinate system (x, y) has its origin at the centroid of face f, marked by an open circle, with x normal to f and y perpendicular to x.

For faces that are far away from the boundaries of a rectangular mesh, we fit the multidimensional polynomial given by equation (4) that has nine unknown coefficients, $\mathbf{a} = a_1 \dots a_9$, using the twelve cell centre values from the upwind-biased stencil, $\phi = \phi_1 \dots \phi_{12}$. This yields a matrix equation

$$
\begin{bmatrix}
1 & x_1 & y_1 & x_1^2 & x_1y_1 & y_1^2 & x_1^3 & x_1^2y_1 & x_1y_1^2 \\
1 & x_2 & y_2 & x_2^2 & x_2y_2 & y_2^2 & x_2^3 & x_2^2y_2 & x_2y_2^2 \\
\vdots & \vdots & \vdots & \vdots & \vdots & \vdots & \vdots & \vdots & \vdots \\
1 & x_{12} & y_{12} & x_{12}^2 & x_{12}y_{12} & y_{12}^2 & x_{12}^3 & x_{12}^2y_{12} & x_{12}y_{12}^2
\end{bmatrix}
\begin{bmatrix}
a_1 \\ a_2 \\ \vdots \\ a_9
\end{bmatrix}
=
\begin{bmatrix}
\phi_1 \\ \phi_2 \\ \vdots \\ \phi_{12}
\end{bmatrix}
\tag{8}
$$

which can be written as

$$
\mathbf{Ba} = \phi \tag{9}
$$

The rectangular matrix $\mathbf{B}$ has one row for each cell in the stencil and one column for each term in the polynomial. $\mathbf{B}$ is called the *stencil matrix,* and it is constructed using only the mesh geometry. A local coordinate system is established in which x is normal to the face f and y is perpendicular to x. The coordinates (x_i, y_i) give the position of the centroid of the ith cell in the stencil. The unknown coefficients $\mathbf{a}$ are calculated using the pseudo-inverse of $\mathbf{B}^+$ found by singular value decomposition:

$$
\mathbf{a} = \mathbf{B}^+\phi \tag{10}
$$

Recall that the approximate value ϕ_F is equal to the constant coefficient a_1, which is a weighted mean of ϕ:

$$
a_1 =
\begin{bmatrix}
b_{1,1}^+ \\ b_{1,2}^+ \\ \vdots \\ b_{1,12}^+
\end{bmatrix}
\cdot
\begin{bmatrix}
\phi_1 \\ \phi_2 \\ \vdots \\ \phi_{12}
\end{bmatrix}
\tag{11}
$$

where the weights $b_{1,1}^+ \dots b_{1,12}^+$ are the elements of the first row of $\mathbf{B}^+$.

In the least squares fit presented above, all stencil values contributed equally to the polynomial fit. Lashley (2002) showed that it is necessary for numerical stability that the polynomial fits the cells connected to face f more closely than other cells in the stencil. To achieve this, we allow each cell to make an unequal contribution to
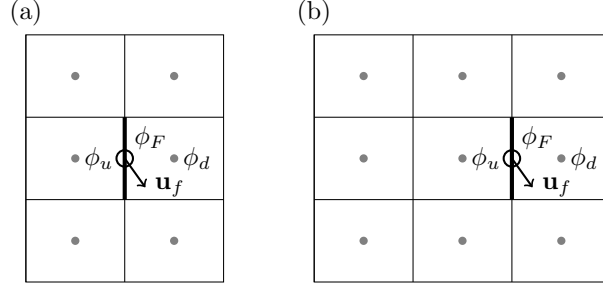
Figure 6: Upwind-biased stencils for faces near the left-hand boundary of a rectangular mesh, with (a) a 2 × 3 stencil for the face immediately adjacent to the left-hand boundary, and (b) a 3 × 3 stencil for the face immediately adjacent to the face in (a). For both stencils, attempting a least squares fit using the nine-term polynomial in equation (4) would result in an underconstrained problem.

the least squares fit. We assign a *multiplier* to each cell in the stencil, $\mathbf{m} = m_1 \ldots m_{12}$, and multiply by equation (9) to obtain

$$\tilde{\mathbf{B}}\mathbf{a} = \mathbf{m} \cdot \phi \tag{12}$$

where $\tilde{\mathbf{B}} = \mathbf{MB}$ and $\mathbf{M} = \mathrm{diag}(\mathbf{m})$. The constant coefficient a_1 is calculated from the pseudo-inverse, $\tilde{\mathbf{B}}^+$:

$$a_1 = \tilde{\mathbf{b}}_1^+ \cdot \mathbf{m} \cdot \phi \tag{13}$$

where $\tilde{\mathbf{b}}_1^+ = \tilde{b}_{1,1}^+ \ldots \tilde{b}_{1,12}^+$ are the elements of the first row of $\tilde{\mathbf{B}}^+$. Again, a_1 is a weighted mean of ϕ, where the weights are now $\tilde{\mathbf{b}}_1^+ \cdot \mathbf{m}$.

For faces of a non-rectangular mesh, or faces that are near a boundary, the number of stencil cells and number of polynomial terms may differ: a stencil will have two or more cells and, for two-dimensional meshes, its polynomial will have between one and nine terms. Additionally, the polynomial cannot have more terms than its stencil has cells because this would lead to an underconstrained system of equations. The procedure for choosing suitable polynomials is discussed next.

3.3 Polynomial generation

The majority of faces on a uniform two-dimensional mesh have stencils with more than nine cells. For example, a triangular mesh has 19 points (figure 4a), a rectangular mesh has 12 points (figure 4b), and a hexagonal mesh has 10 points (figure 4c). In all three cases, constructing a system of equations using the nine-term polynomial in equation (4) leads to an overconstrained problem that can be solved using least squares. However, this is not true for faces near boundaries: stencils that have fewer than nine cells (figure 6a) would result in an underconstrained problem, and stencils that have exactly nine cells may lack sufficient information to constrain high-order terms. For example, the stencil in figure 6b lacks sufficient information to fit the x^3 term. In such cases, it becomes necessary to perform a least squares fit using a polynomial with fewer terms.

For every stencil, we find a set of *candidate polynomials* that do not result in an underconstrained problem. In two dimensions, a candidate polynomial has between one and nine terms and includes a combination of the terms in equation (4). There are two additional constraints that a candidate polynomial satisfy.

First, high-order terms may be included in a candidate polynomial only if the lower-order terms are also included. Let

$$M(x, y) = x^i y^j : i, j \geq 0 \text{ and } i + j \leq 3 \tag{14}$$

be the set of all monomials of degree at most 3 in x, y. A subset S of $M(x, y)$ is "dense" if, whenever $x^a y^b$ and $x^c y^d$ are in S with $a \leq c$ and $b \leq d$, then $x^i y^j$ is also in S for all $a < i < c$, $b < j < d$. For example, the polynomial

$\phi = a_1 + a_2 x + a_3 y + a_4 xy + a_5 x^2 + a_6 x^2 y$ is a dense subset of $M(x, y)$, but $\phi = a_1 + a_2 x + a_3 y + a_4 x^2 y$ is not because $x^2 y$ can be included only if xy and x^2 are also included.

Second, a candidate polynomial must have a stencil matrix $\mathbf{B}$ that is full rank. The matrix is considered full rank if its smallest singular value is greater than 1×10^{-9}. Using a polynomial with all nine terms and the stencil in figure 6b results in a rank-deficient matrix and so the nine-term polynomial would not be a candidate polynomial.

The candidate polynomials are all the dense subsets of $M(x, y)$ that have a stencil matrix that is full rank. The final stage of the advection scheme selects a candidate polynomial and ensures that the least squares fit is numerically stable.

3.4 Stabilisation procedure

So far, we have constructed a stencil and found a set of candidate polynomials. Applying a least squares fit to any of these candidate polynomials avoids creating an underconstrained problem. The final stage of the advection scheme chooses a suitable candidate polynomial and appropriate multipliers so that the fit is numerically stable.

The approximated value ϕ_F is equal to a_1 which is calculated from equation (13). The value of a_1 is a weighted mean of ϕ where $\mathbf{w} = \tilde{\mathbf{b}}_1^+ \cdot \mathbf{m}$ are the weights. If the cell centre values ϕ are assumed to approximate a smooth field then we expect ϕ_F to be close to the values of ϕ_u and ϕ_d, and expect ϕ_F to be insensitive to small changes in ϕ. When the weights $\mathbf{w}$ have large magnitude then this is no longer true: ϕ_F becomes sensitive to small changes in ϕ which can result in large departures from the smooth field ϕ.

A one-dimensional von Neumann analysis was performed to obtain stability constraints on the weights $\mathbf{w}$. The analysis is presented in the appendix, and it shows that the weights must satisfy three constraints:

$$0.5 \leq w_u \leq 1 \tag{15a}$$

$$0 \leq w_d \leq 0.5 \tag{15b}$$

$$w_u - w_d \geq \max_{p \in P}(|w_p|) \tag{15c}$$

where w_u and w_d are the weights for the upwind and downwind cells respectively. The *peripheral cells P* are the cells in the stencil that are not the upwind or downwind cells, and w_p is the weight for a given peripheral cell p.

The stabilisation procedure comprises three steps. In the first step, the candidate polynomials are sorted in preference order so that candidates with the most terms are preferred over those with fewer terms. If there are multiple candidates with the same number of terms, the candidate with the largest minimum singular value is preferred. This ordering ensures that the preferred candidate is the highest-order polynomial with the most information content.

In the second step, the most-preferred polynomial is taken from the list of candidates and the multipliers are assigned so that the upwind cell and downwind cell have multipliers $m_u = 1024$ and $m_d = 1024$ respectively, and all peripheral cells have multipliers $m_p = 1$. This choice results in a least squares fit in which the polynomial passes almost exactly through the upwind and downwind cell centre values.

In the third step, we calculate the weights $\mathbf{w}$ from the least squares fit and evaluate them against the stability constraints given in equation (15). If any constraint is violated, the value of m_d is halved and the constraints are evaluated with the new weights. This step is repeated until the weights satisfy the stability constraints, or m_d becomes smaller than one. If the constraints are still not satisfied, then we start again from the second step with the next-preferred polynomial in the candidate list.

Finally, if no stable weights are found for any candidate polynomial, we revert to an upwind scheme such that $w_u = 1$ and all other weights are zero. In fact, we have not encountered any stencil for which this last resort is required.

To illustrate the stabilisation procedure, figure 7a presents a one-dimensional example of a cubic polynomial fitted through five points, with the weight at each point printed above it. In preference order, the candidate
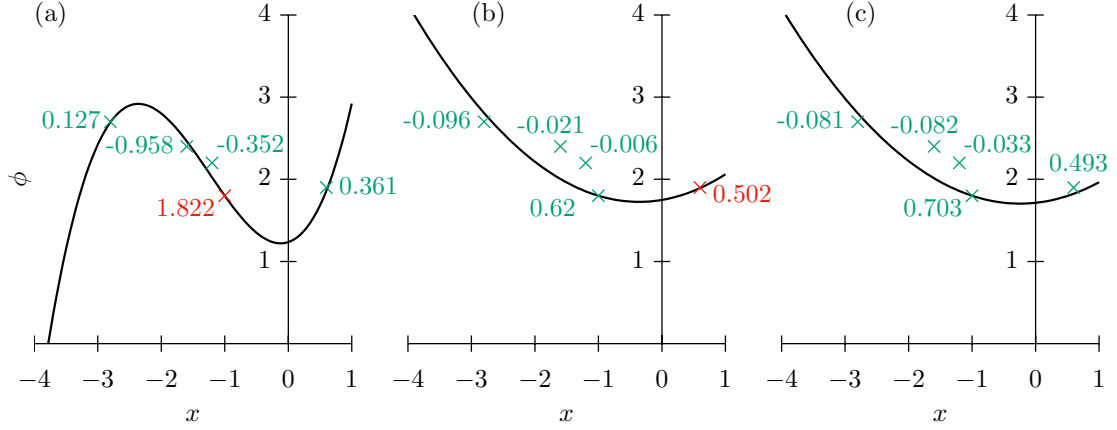
Figure 7: A one-dimensional least squares fits to a stencil of five points using (a) a cubic polynomial with multipliers $m_u = 1024$, $m_d = 1024$ and $m_p = 1$, (b) a quadratic polynomial with the same multipliers, and (c) a quadratical polynomial with multipliers $m_u = 1024$, $m_d = 1$ and $m_p = 1$. Notice that the curves in (a) and (b) fit almost exactly through the upwind and downwind points immediately adjacent to the y-axis, but in (c) the curve fits almost exactly only through the upwind point immediately to the left of the y-axis. The point data are labelled with their respective weights. Points that have failed one of the stability constraints in equation (15) are marked in red. The upwind point is located at $(-1, 1.8)$ and the downwind point at $(0.62, 1.9)$, and the peripheral points are at $(-2.8, 2.4)$, $(-1.6, 2.7)$ and $(-1.2, 2.2)$.

polynomials are

$$\phi = a_1 + a_2 x + a_3 x^2 + a_4 x^3 \tag{16}$$

$$\phi = a_1 + a_2 x + a_3 x^2 \tag{17}$$

$$\phi = a_1 + a_2 x \tag{18}$$

$$\phi = a_1 \tag{19}$$

We begin with the cubic equation. The multipliers are chosen so that the polynomial passes almost exactly through the upwind and downwind points that are immediately to the left and right of the y-axis respectively. The constraint on the upwind point is violated because $w_u = 1.822 > 1$ (equation 15a). Reducing the downwind multiplier does not help to satisfy the constraint, so we start again with the quadratic equation (figure 7b). Again, the multipliers are chosen to force the polynomial through the upwind and downwind points, but this violates the constraint on the downwind point because $w_d = 0.502 > 0.5$ (equation 15b). This time, however, stable weights are found by reducing w_d to one (figure 7c) and these are the weights that will be used to approximate ϕ_F, where the polynomial intercepts the y-axis.

Appendix: One-dimensional von Neumann stability analysis

Two analyses are performed in order to find stability constraints on the weights $\mathbf{w} = \tilde{\mathbf{b}}_1^+ \cdot \mathbf{m}$ as appear in equation (13). The first analysis uses two points to derived separate constraints on the upwind weight w_u and downwind weight w_d. The second analysis uses three points to derive a constraint that considers all weights in a stencil.

Two-point analysis

We start with the conservation equation for a dependent variable ϕ that is discrete-in-space and continuous-in-time

$$\frac{\partial \phi_j}{\partial t} = -u \frac{\phi_R - \phi_L}{\Delta x} \tag{20}$$

where the left and right fluxes, ϕ_L and ϕ_R are weighted averages of the neighbouring points. Assuming that u is positive

$$\phi_L = \alpha_u \phi_{j-1} + \alpha_d \phi_j \tag{21}$$
$$\phi_R = \beta_u \phi_j + \beta_d \phi_{j+1} \tag{22}$$

where α_u and β_u are the upwind weights and α_d and β_d are the downwind weights for the left and right fluxes respectively. A subscript j denotes the value at a given point $x = j\Delta x$ where Δx is a uniform mesh spacing.

At a given time $t = n\Delta t$ at time-level n and with a time-step Δt, we assume a wave-like solution with an amplification factor A, such that

$$\phi_j^{(n)} = A^n e^{ijk\Delta x} \tag{23}$$

where $\phi_j^{(n)}$ denotes a value of ϕ at position j and time-level n. Using this to rewrite the left-hand side of equation (20)

$$\frac{\partial \phi_j}{\partial t} = \frac{\partial}{\partial t} \left(A^{t/\Delta t} \right) e^{ijk\Delta x} = \frac{\ln A}{\Delta t} A^n e^{ikj\Delta x} \tag{24}$$

hence equation (20) becomes

$$\frac{\ln A}{\Delta t} = -\frac{u}{\Delta x} \left(\beta_u + \beta_d e^{ik\Delta x} - \alpha_u e^{-ik\Delta x} - \alpha_d \right) \tag{25}$$
$$\ln A = -c \left(\beta_u - \alpha_d + \beta_d \cos k\Delta x + i\beta_d \sin k\Delta x - \alpha_u \cos k\Delta x + i\alpha_u \sin k\Delta x \right) \tag{26}$$

where the Courant number $c = u\Delta t/\Delta x$. Let $\Re = \beta_u - \alpha_d + \beta_d \cos k\Delta x - \alpha_u \cos k\Delta x$ and $\Im = \beta_d \sin k\Delta x + \alpha_u \sin k\Delta x$, then

$$\ln A = -c \left(\Re + i\Im \right) \tag{27}$$
$$A = e^{-c\Re} e^{-ic\Im} \tag{28}$$

and the complex modulus and complex argument of A are found to be

$$|A| = e^{-c\Re} = \exp\left(-c \left(\beta_u - \alpha_d + (\beta_d - \alpha_u) \cos k\Delta x \right)\right) \quad \text{and} \tag{29}$$
$$\arg(A) = -c\Im = -c \left(\beta_d + \alpha_u \right) \sin k\Delta x \tag{30}$$

For stability, we need $|A| \leq 1$ and $\arg(A) < 0$ for $c > 0$, so

$$\beta_u - \alpha_d + (\beta_d - \alpha_u) \cos k\Delta x \geq 0 \quad \forall k\Delta x \quad \text{and} \tag{31}$$
$$\beta_d + \alpha_u > 0 \tag{32}$$

Imposing the additional constraints that $\alpha_u = \beta_u$ and $\alpha_d = \beta_d$:

$$|A| = \exp\left(-c \left(\alpha_u - \alpha_d \right) (1 - \cos k\Delta x)\right) \tag{33}$$

and given $1 - \cos k\Delta x \geq 0$ for well-resolved waves, then

$$\alpha_u - \alpha_d \geq 0 \tag{34}$$

which provides a lower bound on α_u:

$$\alpha_u \geq \alpha_d \tag{35}$$

Additionally, we do not want more damping than an upwind scheme (where $\alpha_u = \beta_u = 1$, $\alpha_d = \beta_d = 0$), having an amplification factor, A_{up}:

$$|A_{\mathrm{up}}| = \exp\left(-c\left(1 - \cos k\Delta x\right)\right) \tag{36}$$

So we need $|A| \geq |A_{\mathrm{up}}|$:

$$-c\left(\alpha_u - \alpha_d\right)\left(1 - \cos k\Delta x\right) \geq -c\left(1 - \cos k\Delta x\right) \tag{37}$$

$$\alpha_u - \alpha_d \leq 1 \tag{38}$$

$$\alpha_u \leq 1 + \alpha_d \tag{39}$$

which provides an upper bound on α_u. Combining with eqn (35) we can bound α_u on both sides:

$$\alpha_d \leq \alpha_u \leq 1 + \alpha_d \tag{40}$$

Now, assume that $\alpha_u + \alpha_d = 1$ (or $\alpha_d = 1 - \alpha_u$), then

$$1 - \alpha_u < \alpha_u \leq 1 + (1 - \alpha_u) \tag{41}$$

$$0.5 \leq \alpha_u \leq 1 \tag{42}$$

and, since $\alpha_u + \alpha_d = 1$, then

$$0 \leq \alpha_d \leq 0.5 \tag{43}$$

Three-point analysis

We start again from equation (20) but this time approximate ϕ_L and ϕ_R using three points:

$$\phi_L = \alpha_{uu}\phi_{j-2} + \alpha_u\phi_{j-1} + \alpha_d\phi_j \tag{44}$$

$$\phi_R = \alpha_{uu}\phi_{j-1} + \alpha_u\phi_j + \alpha_d\phi_{j+1} \tag{45}$$

having used the same weights α_{uu}, α_u and α_d for both left and right fluxes. Substituting equation (23) into equation (20) we find

$$A = \exp\left(-c\left[\alpha_{uu}\left(e^{-ik\Delta x} - e^{-2ik\Delta x}\right) + \alpha_u\left(1 - e^{-ik\Delta x}\right) + \alpha_d\left(e^{ik\Delta x} - 1\right)\right]\right) \tag{46}$$

So that, if the complex modulus $|A| \leq 1$ then

$$\alpha_u - \alpha_d + \left(\alpha_{uu} - \alpha_u + \alpha_d\right)\cos k\Delta x - \alpha_{uu}\cos 2k\Delta x \geq 0 \tag{47}$$

If $\cos k\Delta x = -1$ and $\cos 2k\Delta x = 1$ then $\alpha_u - \alpha_d \geq \alpha_{uu}$, and if $\cos k\Delta x = 0$ and $\cos 2k\Delta x = -1$ then $\alpha_u - \alpha_d \geq -\alpha_{uu}$. Hence we find that

$$\alpha_u - \alpha_d \geq |\alpha_{uu}| \tag{48}$$

and, when the same analysis is performed with four points, α_{uuu}, α_{uu}, α_u and α_d, we find that the same condition holds replacing α_{uu} with α_{uuu}. Hence, we generalise equation (48) to find the final stability constraint

$$\alpha_u - \alpha_d \geq \max_{p \in P}|\alpha_p| \tag{49}$$

where the peripheral cells P is the set of all stencil cells except for the upwind and downwind cell, and α_p is the weight for a given peripheral cell p.